analytical chemistry

ARTICLE

pubs.acs.org/ac

# MicroRNA Profiling by Simultaneous Selective Isotachophoresis and Hybridization with Molecular Beacons

Alexandre Persat and Juan G. Santiago*

Department of Mechanical Engineering, Stanford University, Stanford, California 94305, United States

Supporting Information

**ABSTRACT:** We present and demonstrate a novel assay for the detection and quantification of microRNA (miRNA) that leverages isotachophoresis (ITP) and molecular beacon (MB) hybridization. We use ITP to selectively preconcentrate miRNA from total RNA. We simultaneously focus MBs and use the ITP zone as a 10 pL reactor with active mixing where MBs fluoresce upon hybridization to target miRNA. To increase both sensitivity and selectivity, we leverage a multistage ITP strategy composed of three discrete regions of different concentrations of denaturant, sieving matrix, and magnesium chloride. We show that ITP hybridization is specific and selective to the miRNA target. We demonstrate ITP hybridization of miRNA in a biologically relevant case by detecting and quantifying miR-122 in human kidney and liver. ITP hybridization is a cheap, simple, high-speed, and amplification-free miRNA profiling method which requires small amounts (order 100 ng) of sample. The technique therefore represents an attractive alternative to PCR or Northern blot for miRNAs.

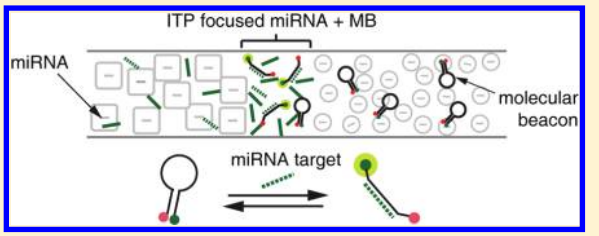


MicroRNAs (miRNAs) are small (~22 nucleotides), non-coding RNA molecules that regulate gene expression.[1] Sequence-specific binding of miRNAs to target mRNA transcripts induces gene silencing, via the formation of the RNA-induced silencing complex (RISC). miRNAs play an important role in gene regulation, both in normal pathology and disease, and therefore constitute a marker for diverse cellular processes.[1] In particular, profiling miRNA is potentially a powerful diagnostics and monitoring tool for cancer.[2,3] Novel and improved techniques for the isolation, detection, and quantification of miRNAs are currently essential to unravel the functions and mode of actions of these small molecules whose analysis by traditional techniques is still limited.[4,5]

The most popular and well-established miRNA profiling methods are adapted from traditional nucleic acid analysis techniques.[4] These include Northern blot, microarrays, sequencing, and reverse-transcription PCR (RT-PCR). Microarrays and sequencing platforms have high throughput but require significant instrumentation and amount of sample (about 5 $\mu$g of total RNA), are time-consuming, and require preamplification which yields significant sequence bias.[4,6] RT-PCR[7] has high dynamic range and is sensitive but has low throughput and is less specific than standard PCR.[4] Lastly, Northern blot has moderate sensitivity and allows for length discrimination of sequences but remains time-consuming and requires large amounts of sample (often >1 $\mu$g of total RNA). Northern blotting consists of gel electrophoresis for separation of total RNA with subsequent transfer to a nitrocellulose membrane, followed by hybridization with a radioactively labeled probe visualized with a scintillation counter.[8] We here adopt a different hybridization strategy which leverages isotachophoresis (ITP) and hybridization with molecular beacons (MBs) for the profiling of miRNA. Our assay is a single, amplification-free process which simultaneously purifies, preconcentrates, actively mixes, hybridizes, and produces an optical signal whose intensity increases with the initial target sample concentration.

Molecular beacons are sequence-specific nucleic acid probes that fluoresce upon hybridization.[9] Developed in the early years of quantitative PCR, molecular beacons have become ideal sequence-specific fluorescent reporters for nucleic acid amplifications assays and In Vivo hybridization.[9,10] The sequence-specific fluorescence of MBs originates from their unique structure shown in Figure 1c. MBs are composed of four units: (i) a nucleic acid probe sequence (the loop, up to about 30 nt long) complementary to the target sequence of interest; this sequence is flanked by (ii) two, complementary self-hybridizing sequences which allow conformation of the probe into a hairpin structure, (iii) a fluorophore at the 5′ end, and (iv) a suitable quencher at the 3′ end. We present a schematic of the MB hybridization reaction mechanism in Figure 1c. When the molecular beacon is free in solution, it acquires a hairpin structure which brings 5′ and 3′ ends to proximity, so the quencher hampers fluorescence. In the presence of a sequence complementary to the probe, the hairpin opens and hybridizes to the target. This is thermodynamically favorable because the short stem hybrid is less stable than the longer probe−target hybrid. In this configuration, the distance between fluorophore and quencher is sufficient to enable fluorescence.

**Received:** December 9, 2010
**Accepted:** January 23, 2011
**Published:** February 18, 2011

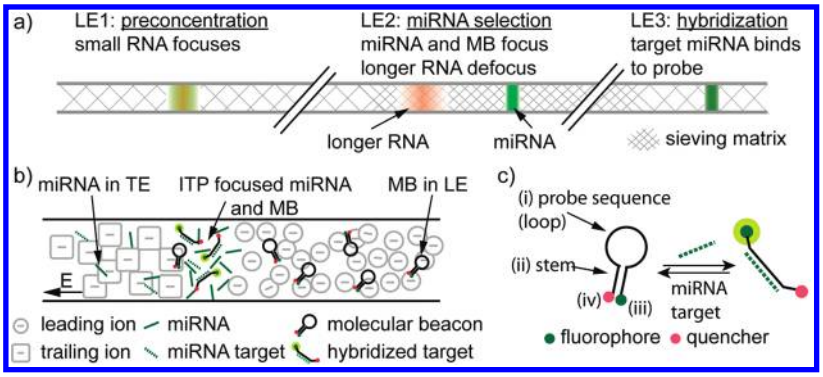


**Figure 1.** Schematic representation of components of the ITP hybridization assay. (a) Schematic of the three-stage ITP strategy used for purification and hybridization. We initially setup three contiguous zones of LE mixes with varying concentrations of polymer, denaturant, leading ion, and magnesium chloride. The first zone LE1 allows for strong preconcentration of small RNA. The second has higher polymer concentration (shown by increased density of cross-hatching) to selectively focus miRNA. LE3 has reduced denaturing conditions to allow for specific hybridization and increased quantum yield of fluorophore. (b) Schematic demonstrating how MB can be integrated in ITP focusing. Targets (miRNA in this work) are initially in the TE and MB in all three LE zones. In the frame of reference of the ITP interface, both MB and target electromigrate toward the interface between TE and LE ions. Probe and target hybridize preconcentrate and mix in the same zone, and hybridization generates a sequence-specific fluorescence signal in the focused zone. (c) Depiction of the structure and mode of action of molecular beacon probes. MBs are DNA molecules with a probe sequence complementary to the target of interest (i), flanked by two segments complementary to each other (ii). The complementary ends are labeled with a fluorophore (iii) and a quencher (iv). In absence of target, the self-complementary flanking sequences hybridize to form a stem and "hairpin" conformation where the quencher's proximity inhibits fluorophore emission. In the presence of a complementary target sequence, the MB opens to form a probe−target hybrid, increases the distance between the fluorophore and quencher, and produces a sequence-specific, quantitative fluorescence signal.

Isotachophoresis is an electrophoretic preconcentration technique which focuses charged species in an inhomogeneous buffer system.[11] Generation of gradients of chemical potentials induces focusing of ionic species whose mobilities range between that of the trailing and the leading electrolyte (TE and LE) co-ions. Species whose mobility is outside the TE-to-LE ion mobility range will not focus.[12] ITP is commonly used as a sample preconcentration technique prior to capillary electrophoresis,[13,14] or as a standalone separation method.[15] More recently, we have leveraged the selectivity of ITP focusing for the purification of nucleic acids[12,16] and the measurement of global miRNA abundance in diverse tissues.[17] To our knowledge, ITP has been utilized only a few times to perform chemical reactions. Park et al. controlled immunoassays by ITP focusing of antibody and antigen prior separation.[18] Persat et al. proposed ITP as a method of controlling isothermal, chemical cycling PCR (including ITP hybridization/annealing and extension) and showed preliminary data.[19] Goet et al. described ITP as a way of bringing and mixing reagents together and discussed DNA hybridization coupled with ITP but did not present an experimental demonstration.[20] Recently, one of us (J.G.S.) and co-workers[21] showed a preliminary demonstration combining ITP and MB hybridization to identify rRNA sequences in urine samples.

In the present work, we combine selective ITP extraction and purification with MB hybridization for the sequence-specific detection of miRNA. In the same manner as our previous work on global (not sequence-specific) mature miRNA quantification,[17] we use a multistage ITP injection strategy to accomplish sensitive, selective, and specific detection. This multistage process achieves high sensitivity in an initial step, high selectivity in a second step, and conditions optimal for sensitive optical detection and hybridization in a third step. We first summarize and discuss experimental conditions of the multistage ITP hybridization assay. Then we demonstrate hybridization and show selectivity and specificity of the assay using synthetic miRNAs. We finally apply the ITP hybridization to a biologically relevant case by detecting and quantifying a specific miRNA in human liver.

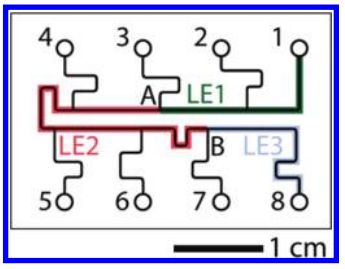


**Figure 2.** Schematic of the zones containing the initial three LE mixtures in the commercial microchip used in this work. We create the initial zones (see Table 2 and Materials and Methods) in the 12 $\mu$m deep, 44 $\mu$m wide wet-etched borosilicate glass microchannel connecting reservoirs 1 and 8. Before each experiment, we fill the microchannels with LE1, LE2, and LE3 according to the sequence described in Table 2. The three LE zones are highlighted for clarity. LE1 (green) and LE2 (red) zones meet at point A, and LE2 and LE3 (gray) meet at B.

**Description of the Assay.** We leverage the selectivity of ITP focusing to perform hybridization solely on the RNA length range of interest. We have used this feature of ITP to quantify global miRNA levels in diverse cell cultures.[17] Here, we selectively focus mature miRNA (18 to 24 nt) and reject all RNA molecules longer than 60 nt from the ITP zone. We therefore avoid bias from hybridization of long RNAs that contain identical or similar sequences; in particular, we exclude the 70 nt long miRNA precursors pre-miRNA.[1] This selectivity combined with the simultaneous hybridization is in some ways similar to the process of Northern blotting, which requires multiple successive steps including electrophoresis and hybridization to achieve detection. In contrast to Northern blotting, ITP here provides simultaneous preconcentration and active mixing of target and probe prior to and during detection.

We use a multizone ITP process which yields both specificity and sensitivity in the initial miRNA purification process. We used

**Table 1. Sequences of Oligoribonucleotides and Molecular Beacons Used in This Work[a]**

| oligo name (length) | sequence (5′ to 3′) |
|---|---|
| miR-26a (22 nt) | UUCAAGUAAUCCAGGAUAGGCU |
| miR-126 (22 nt) | UCGUACCGUGAGUAAUAAUGCG |
| miR-122 (22 nt) | UGGAGUGUGACAAUGGUGUUUG |
| mir-26a (77 nt) | GUGGCCUCGUUCAAGUAAUCCAGGAUAGGCUGUGCAGGU |
| (miR-26a precursor) | CCCAAUGGGCCUAUUCUUGGUUACUUGCACGGGGACGC |
| miR-26a MB (34 nt) | TYE665 - CCGAGCAGCCTATCCTGGATTACTTGAAGCTCGG - IBRQ |
| miR-122 MB (34 nt) | TYE665 - CCGAGCCAAACACCATTGTCACACTCCAGCTCGG - IBRQ |

[a] For molecular beacons, TYE 665 is a fluorophore (with spectrum similar to Cy5) and Iowa Black RQ (IBRQ) is the quencher. miRNAs and precursor are ribonucleic acids while molecular beacons are deoxyribonucleic acids. For molecular beacons, the complementary stem-forming sequence fragments are underlined.

a similar purification strategy in previous work on miRNA,[17] where the zones allowed for successive preconcentration, selection, and quantification of global miRNA. We created three initial contiguous LE zones arranged in series along the separation channel. Initial LE zones had distinct initial concentrations of (the same) leading ion, polymer sieving matrix, or denaturant. As ITP proceeds, the nucleic acid sample trails leading ions as ions migrate through the successive, stationary zones of denaturant and sieving matrix (which have zero electrophoretic mobility). Here, we combine highly selective purification and preconcentration with a novel hybridization strategy. We use three successive zones to preconcentrate small RNA, select miRNA, and hybridize and detect a specific target with MBs in the ITP zone.

The function of each step is summarized in Figure 1a. The sample is mixed in the TE which includes 5 mM MOPS, 5 mM Tris, and 92.5% v/v formamide. TE and sample are loaded into the sample reservoir 1 of Figure 2. In the first zone LE1, we use a low (0.5% w/v PVP) sieving matrix polymer concentration and 7 M urea. The mobility of miRNA increases with decreasing polymer concentration, so LE1 yields a strong flux of RNA to the ITP interface, but molecules longer than (mature) miRNA molecules are also focused. Also, the slightly larger concentration of leading ions in LE1 (50 mM) augments ITP preconcentration dynamics.[22] The second zone LE2 has large polymer concentration (3% w/v PVP), which globally decreases mobility of RNA. This defocuses longer RNA (they fall behind and out of the ITP focus zone) while leaving miRNA and MB focused, at the cost of locally retarding focusing dynamics. As discussed below, the cutoff length is below 60 nt, so that miRNAs can focus, but pre-miRNAs cannot focus. Finally, LE3 has low denaturing conditions (2 M urea, lower polymer concentration of 0.5% w/v), and optimized magnesium chloride concentration (2 mM $Mg^{2+}$). These conditions enable fast hybridization and optimize fluorescence signals as miRNAs specifically bind to MBs.

We show a detailed view of the final ITP hybridization step (occurring in LE3 zone) in Figure 1b. Initially, MB probes targeting the miRNA of interest are dissolved in the three LEs, and total RNA (which includes miRNA) is dissolved in the TE. Leading and trailing ions are selected so that their mobilities allow for simultaneous and colocated focusing of miRNA, MB probe, and the miRNA−probe hybrid. (The latter ITP format which focuses multiple analytes into a common, sharp zone is called peak mode ITP.[23]) Under this condition, miRNA and MB and the hybrid simultaneously focus at the interface between TE and LE. In the laboratory frame, miRNA overspeed the TE ions and other RNA and migrate toward the ITP zone. At the same time, the ITP zone overtakes and focuses MBs initially in the LE, so target and probe are actively preconcentrated and driven into ITP zone. In this focused zone, and under optimized conditions, miRNA hybridizes to the probe sequence of the MB, disrupting their hairpin structure and yielding a sequence-specific increase in fluorescence intensity within this ITP zone. This way, the focused zone acts as a reactor volume defined by its axial width and the cross-sectional area of the microchannel. In our 44 $\mu$m wide, 12 $\mu$m deep channel, we estimate the volume of the ITP reaction zone to be on the order of 10 pL, given our observed ~10 $\mu$m wide ITP interfaces.[23] This is a significantly smaller reaction volume compared to existing microfluidic reactors, which are at least on the order of a few nanoliters.[24] The strong preconcentration dynamics (we estimate order $10^3$ to $10^4$ fold increase of reactants in our conditions) yield improved kinetics and sensitivity.

## MATERIALS AND METHODS

**Chemicals and Reagents.** Leading electrolytes contain DNase- and RNase-free Tris hydrochloride buffer (pH = 8.0, Invitrogen, Carlsbad, CA), poly(vinylpyrrolidone) (PVP, MW = 1 000 000, Polysciences Inc., Warrington, PA), urea (EMD biosciences, Gibbstown, NJ), and magnesium chloride (EMD biosciences, Gibbstown, NJ). Concentrations in LE1, LE2, and LE3 are, respectively, 50, 20, and 20 mM of Tris hydrochloride; 0.5% w/v, 3% w/v and 0.5% w/v of PVP; 7, 7, and 2 M of urea; 0, 2, and 2 mM of magnesium chloride. The TE is a solution of 5 mM Tris (Sigma-Aldrich, Saint Louis, MO) and 5 mM MOPS (Sigma-Aldrich) in 92.5% v/v formamide (UltraPure, Invitrogen). All solutions were prepared with DNase- and RNase-free deionized water (Gibco, Carlsbad, CA).

We purchased HPLC-purified molecular beacons and synthetic miRNA from Integrated DNA Technologies (Coralville, IA). We used (DNA) molecular beacons, 5′-labeled with TYE 665 fluorescent dye (excitation at 645 nm and emission at 665 nm) and 3′-labeled with Iowa Black RQ quencher (peak absorbance at 656 nm). The precursor mir-26a was synthesized and PAGE-purified by Dharmacon (Lafayette, CO). We provide the sequences of synthetic oligoribonucleotides and probes used in this work in Table 1. Total RNA from normal human liver and kidney were obtained from Ambion (FirstChoice human total RNA, Austin, TX). Before each experiment, we dissolved the sample (total or synthetic RNA) to the specified concentration in 50 $\mu$L of TE, placed in a water bath at 70 °C for 5 min and finally on ice until running the ITP hybridization experiment. Separately, we dissolved the MB in 500 $\mu$L of each LE.

**ITP Protocol.** We here describe the injection protocol to perform the three-stage ITP hybridization. We performed all

**Table 2. Summary of the Injection Protocol**

| | reservoir | | | | | | | |
|---|---|---|---|---|---|---|---|---|
| | 1 | 2 | 3 | 4 | 5 | 6 | 7 | 8 |
| step 1 | LE1, 5 $\mu$L | LE1, 5 $\mu$L | LE1, 5 $\mu$L | LE2, 5 $\mu$L | LE2, 5 $\mu$L | LE2, 5 $\mu$L | LE3, 5 $\mu$L | LE3, 10 $\mu$L |
| step 2 | | | vacuum 2 min | | | | vacuum 2 min | |
| step 3 | empty, rinse, add 10 $\mu$L TE+sample | | | | | | | |
| step 4 | GND | | | | | | | +3 kV |

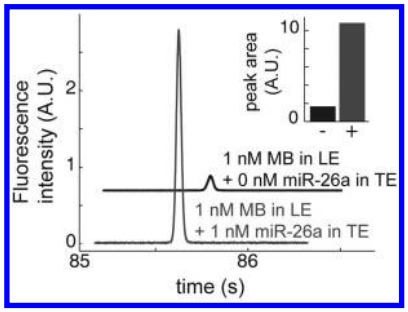


**Figure 3.** Initial demonstration of the ITP hybridization assay. We show two isotachopherograms acquired 8 mm into the LE3 zone. In both experiments, the LE contains 1 nM of MB targeting miR-26a. The upper black trace corresponds to a negative control experiment where the TE contains no RNA. This trace exhibits a peak which we attribute to imperfect quenching of the focused MB. The gray trace shows the result of ITP-hybridization where we added 1 nM of miR-26a target to the TE. The ITP peak has significantly greater amplitude compared to the negative control. This demonstrates successful combination of ITP- and MB-based hybridization for the detection of miRNA. We report the area of each peak in the inset. The peak area of this experiment with 1 nM target in the TE (+) is more than 6 times larger than the area of the negative control (−). The black trace is displaced +0.5 s and +0.7 A.U. on the plot for clarity of presentation.

experiments in an off-the-shelf borosilicate glass microfluidic chip (model NS260, Caliper LS, Mountain View, CA) whose design is shown in Figure 2. Its multiple T-junctions enable generation of the initial serial LE zones by vacuum filling. Initially we precondition the chip by successively flushing channels with 200 mM sodium hydroxide (5 min), deionized (DI) water (1 min), 100 mM hydrochloric acid (5 min), and again DI water (1 min). We then deliver LE1 to reservoirs 1, 2, and 3, LE2 to reservoirs 4, 5, and 6, and LE3 to reservoirs 7 and 8. We subsequently apply vacuum to reservoirs 3 and 7 for 5 min. These preliminary steps help to reduce electroosmotic flow in the borosilicate chip for subsequent experiments.

Before each experiment, all reservoirs are rinsed with DI water. We then deliver LEs to the reservoirs as described above and in Table 2 and apply vacuum to reservoirs 3 and 7 for 2 min. Vacuum at reservoir 3 generates the interface between LE1 and LE2 at the intersection A (see Figure 2) and vacuum at reservoir 7 creates an interface between LE2 and LE3 at the intersection B. After loading, we release both vacuum connections, rinse reservoir 1 with DI water, and deliver the mixture of TE and sample. We generate an electric field in the separation channel by applying a 3 kV voltage difference between reservoirs 8 and 1 using a high voltage power supply (Labsmith, Livermore, CA). This activates ITP focusing and migration of miRNA and MBs through the three serial zones. We eventually stop voltage after the ITP interface has passed the detector which monitors fluorescence in the LE3 zone.

**Optical Setup.** We acquired data with an inverted epifluorescence microscope (Eclipse TE200, Nikon, Japan) equipped with a laser diode illumination (642 nm, Stradus 642, Vortran, Sacramento, CA). Light was filtered using a standard Cy5 cube (exciter/emitter 630/695 nm, model XF110-2, Omega Optical, Brattleboro, VT) and focused though a 60× water immersion objective (N.A. = 1.0, Fluor, Nikon, Japan). To reduce noise from out of focus light sources, we built a custom confocal assembly by placing a 150 $\mu$m pinhole (mounted precision pinhole, Edmund Optics, Barrington, NJ) at the image focal plane. We measured fluorescence intensity using a photomultiplier tube (PMT, model H7422-40, Hamamatsu Photonics, Japan) with voltage set to 900 V. We converted the PMT signal using an amplifier/converter unit (C7319, Hamamatsu, Japan) and filtered it with a simple low pass RC circuit (RC = 1.2 ms). We acquired the resulting voltage signal with a DAQ card (NI USB-6211, National Instruments, Austin, TX) controlled with Matlab (The Mathworks, Natick, MA). We performed all measurements at 250 kS/s data rate and applied a 4000 points moving average to the signal for analysis. We processed the voltage trace by fitting a Gaussian function to the ITP peak. We then calculated fluorescence intensity by integrating the raw data under the fit over three standard deviations. Uncertainty bars determined from $N$ = 4 samples per condition and represent 95% confidence on the mean, calculated assuming a Student's $t$-distribution.

## RESULTS AND DISCUSSION

**Initial Demonstration Using Synthetic miRNA.** We present a typical ITP hybridization assay in Figure 3. We perform the multistage ITP with 1 nM of MB targeting miR-26a in all three LEs. We compare the signal of an ITP assay where the TE contains 1 nM synthetic miR-26a to a negative control (with no target in the TE). We show the two resulting isotachopherograms (fluorescence versus time) in Figure 3. The (top) black trace corresponds to the fluorescence intensity of the negative control. This trace exhibits a signal peak which we attribute to residual fluorescence from incomplete quenching of focused MB.[25] In the experiment where the TE contains 1 nM of miR-26a (gray trace), the fluorescence signal in the ITP zone increases significantly. This shows successful hybridization of the target and MBs within the focused zone. To compare the two results, we calculated the corresponding peak areas and report them in the inset as a bar diagram. The peak area of the hybridized peak (+) is here about 6.5 larger than the one of the negative control (−).

For an ITP hybridization experiment with a peak area $A$, we define the relative fluorescence enhancement $f$ as:

$$f = \frac{A}{A_{nc}} - 1$$


dx.doi.org/10.1021/ac103225c |Anal. Chem. 2011, 83, 2310–2316

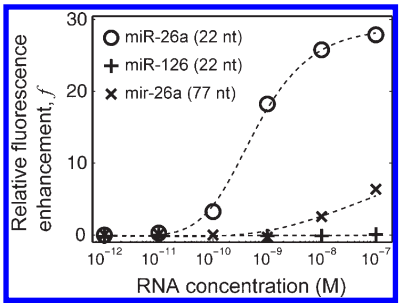


**Figure 4.** Demonstration of specificity and selectivity of the ITP hybridization assay. We performed ITP hybridization with MBs targeting miR-26a and where the TE contains miR-26a (circles), miR-126 (plus), or mir-26a (cross) at concentrations ranging from 1 pM to 100 nM. We here report relative fluorescence enhancement $f$ as defined in the text. To aid in data visualization, we fitted the data with spline functions (dashed lines). Titration with miR-26a shows the signal generated from hybridization of the perfectly matching target. Fluorescence enhancement remains small at low concentration (below 10 pM) and significantly increases at 100 pM and above. $f$ plateaus over about 10 nM, where nearly all focused MBs are open. We also verified potential unspecific hybridization by titrating with miR-126 (whose sequence is distinct from miR-26a) and observed that fluorescence enhancement remained approximately null at all concentrations. This confirms the specificity of MB hybridization in the ITP zone. Titration with the precursor mir-26a sample shows only slow increase of fluorescence with concentration above 10 nM, since the longer molecules are filtered out by the ITP process. This shows that ITP in the LE2 zone excludes miRNA precursors from the focused zone and allows for selective hybridization on miRNA.

where $A_{nc}$ is the peak area of the negative control, i.e., an experiment with equal MB concentration but a blank TE. In the case presented in Figure 3, $f$ is approximately 5.5. $f$ theoretically varies between zero (when $A = A_{nc}$) and a saturation value where all focused MB are open. The latter occurs when the number of target copies in the focused zone is much larger than the number of MBs.

Efficiency and speed of hybridization depend on several parameters including temperature, ion concentration, and target sequence; for example, see Straus et al.[26] Here, hybridization is simultaneous and coupled with the ITP dynamics which preconcentrate beacons and target into the ITP zone. Thus, the hybridization dynamics are also coupled to ITP chemistry and conditions. The dynamics of $f$ therefore depend on at least MB sequence and concentration, choice of fluorophore/quencher pair, temperature, ionic strength, magnesium concentration, ion mobilities (particularly TE ion mobility), applied voltage, and denaturant concentration. Here, we optimized the miRNA hybridization process empirically. Briefly, we first performed a set of control hybridization experiments off-chip using a series of beacon and target concentrations in LE and TE buffers. We quantified fluorescence signals and our signal factor $f$ for these mixtures using a Nanodrop 3300 fluorospectrometer (data not shown). In this calibration, we also varied denaturant and magnesium concentrations and chose concentrations which maximized fluorescence enhancement for the ITP hybridization. We then tested and fine-tuned these chemistries in a series of ITP experiments. We hope to create and present a quantitative model of this complex process in a future paper.

The fluorescence enhancement of MBs increases with target concentration.[25] In peak mode ITP, the amount of focused sample is a linear function of sample concentration in the TE.[23] Consequently, in the ITP hybridization assay, $f$ increases with target concentration in the TE. We performed titration experiments to illustrate the effect of sample concentration on fluorescence enhancement. In Figure 4, we report fluorescence enhancements for ITP hybridization at 100 pM MB with miR-26a concentrations ranging from 1 pM to 100 nM in the TE (circles). At low target concentration, here 1 to 10 pM, the fluorescence enhancement remains negligible. $f$ significantly increases above 100 pM. The most sensitive increase occurs between 100 pM and 1 nM. Above 10 nM, $f$ varies only slightly and seems to reach a plateau value, indicating saturation of MBs. The maximum value of $f$ in this titration experiment is approximately 28 (at 100 nM miR-26a).

**Specificity.** We demonstrate that in ITP hybridization, MBs bind specifically to the correct target sequence. Molecular beacons have intrinsically high specificity, [27] and we confirm here that ITP conditions do not alter this property; we experimentally verify that the detection of the miRNA target is not biased by the presence of other miRNA. To this end, we perform ITP hybridization on a mature miRNA whose sequence does not match the MB probe. We used the MB designed for detection of miR-26a and varied the concentration of a "model" exogenous miRNA in the TE: the mature miRNA sequence miR-126. The resulting titration curve is shown in Figure 4 ("+" symbols). Together with the titration using the correct target (circles), we show titration with the incorrect miRNA sequence miR-126 as a control for hybridization specificity. The miR-126 control shows no increase in fluorescence, demonstrating the specificity of ITP hybridization.

**Selectivity.** We now demonstrate the selectivity (associated here with molecule length) for miRNA of the ITP hybridization assay. Mature miRNAs are generated from processing of longer precursors, successively the pri-miRNA and pre-miRNA. The latter is about 70 nt long and is the shortest precursor preceding full miRNA maturation.[1] Because these precursors contain the mature sequence, hybridization must be carried out exclusively on isolated, shorter miRNA, as in Northern blotting. We achieve this by leveraging the variation of electrophoretic mobility of RNA with length. In a polymer sieving matrix, mobility decreases with increasing polynucleotide length.[28] miRNA is the shortest class of RNA; hence, its mobility is the greatest among all RNA. In particular, it is greater than that of its precursors. Therefore, careful selection of the trailing ion and polymer concentration allow for selective focusing of miRNA, excluding (longer) non-miRNA containing an identical sequence.

To achieve high selectivity, we performed calibration experiments in the same manner as we did in our previous work on miRNA isolation.[17] We first chose an initial trailing ion (here MOPS) and selected a polymer concentration in LE2 that shows focusing of miRNA and MB (separately and simultaneously). We then adjusted LE2 polymer concentration (by increasing from the initial concentration) to reject pre-miRNA from the focused zone while retaining ITP focusing of miRNA and MBs. We found that 3% w/v PVP in LE2 matched this requirement. For the current conditions, we estimate our cutoff length to be about 60 nt (we focus only on shorter RNA).

We also use Figure 4 to illustrate the selectivity of this chemistry by comparing the aforementioned results for the short, mature miR-26a (here the capital "R" indicates a mature sequence, vs the small case "r" which indicates a precursor) to results of focusing a sample of its 77 nt long precursor mir-26a ("x" symbols in Figure 4). The enhancement $f$ for the longer molecule sample mir-26a is globally much smaller than the signal

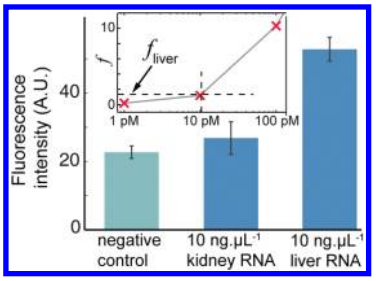


**Figure 5.** Demonstration of ITP hybridization assay for detection and quantification of miR-122 in kidney and liver. We plot peak areas of ITP hybridization experiments where LEs initially contain 100 pM MBs targeting miR-122. The experiments shown have TEs which contain a blank (left bar), 10 ng $\mu L^{-1}$ of total RNA from human kidney (middle bar), and 10 ng $\mu L^{-1}$ of total RNA from human liver (right bar). The increase in fluorescence for kidney over the control is not statistically significant, showing our assay predicts miR-122 concentration in kidney below a limit of detection of 3000 copies per cell. The peak area for liver is significantly greater, indicating greater expression of miR-122. We use a calibration curve built using synthetic miR-122 to estimate target concentration from fluorescence enhancement. The solid gray line in the inset shows a calibration curve resulting from interpolation of hybridization results from synthetic miR-122 versus concentration (red "x" symbols). We use this curve to calculate the concentration corresponding to the enhancement $f_{liver}$ = 1.3. We estimate this concentration to 10.3 pM, corresponding to approximately 16 000 ± 400 copies per cell. Uncertainty bars represent 95% confidence on the mean.

generated by the mature miRNA. $f$ remains at background level equivalent to about 1 nM mir-26a. We note a slight increase of fluorescence enhancement with increasing precursor concentration above 10 nM. We attribute this residual signal to hybridization of byproducts (present at low concentrations) resulting from imperfect RNA synthesis and PAGE purification (purity ~90% according to the manufacturer). These byproducts include short RNA fragments containing segments of the mature sequence, which can hybridize with MB. Our previous work in calibrating the cutoff lengths of this three-zone ITP purification support this conclusion.[17]

Altogether the data show fluorescence in the focused ITP zone is unaffected by nontarget miRNA, and that the MB signal is specific to miR-26a.[29] The length selectivity and sequence specificity of our assay shows its efficacy to precisely detect specific miRNA sequences in total RNA samples.

**miR-122 Profiling in Human Liver with ITP Hybridization.** To show the efficacy of the ITP hybridization assay in a biologically relevant case, we performed detection of miR-122 in two human tissue total RNA samples. We chose the following liver-specific miRNA target for its large dynamic range of expression: miR-122 is highly expressed in liver but poorly expressed in other organs.[30] We diluted total RNA from human liver and kidney in TE down to 10 ng $\mu L^{-1}$. We then performed the ITP hybridization assay on these samples with 100 pM MBs in the LE targeting miR-122. We show a sample isotachopherogram for the detection of miR-122 in liver in Figure S1, Supporting Information.

We show results of these experiments along with a negative control (blank run) in Figure 5, where we report ITP peak areas. ITP hybridization of miR-122 in kidney shows a slight increase in fluorescence ($f$ = 0.2), which is not statistically significant compared to negative control (failed the $t$ test). We conclude that the concentration of miR-122 in kidney is below the limit of detection of our assay. We estimate this limit to 2 pM ($f$ > 0.4, see calibration below), which corresponds to 3000 copies per cell (assuming 25 pg of RNA per cell). This is consistent with the amount of miR-122 measured in mouse kidney by the RNase protection assay.[30] Conversely, ITP hybridization of miR-122 in liver yields significant signal enhancement ($f$ = 1.3 ± 0.15). This indicates that miR-122 is largely expressed in liver compared to kidney, confirming previous reports.[30]

We performed quantification of miR-122 in liver using this measurement and leveraging a calibration curve we built with synthetic miR-122, in the same manner as the calibration of Figure 4. We measured the peak area of ITP hybridization of synthetic oligos dissolved at 1, 10, and 100 pM in the TE. We then performed a linear interpolation between the respective $f$ values to yield a simple relation between fluorescence enhancement and miRNA concentration. We show a portion of this interpolation in the inset of Figure 5 (gray solid line) for concentration values neighboring 10 pM. Using this calibration and the value of $f$ found for liver ($f_{liver}$ in the inset of Figure 5), we calculated that a liver cell contains 16 000 ± 400 copies of miR-122. This is on the same order of magnitude as an RNase protection assay (50 000 copies per cell[30]) or RT-PCR measurements (10 000 copies per 10 pg of RNA or 25 000 copies per cell given our assumption on RNA mass per cell).[31] We believe the slight discrepancy between these three values arises in part from each assay's uncertainty, biological variability, differences in RNA quality,[32] or distinct efficiencies of miRNA extraction methods.[33]

## CONCLUSION

We presented, characterized, and demonstrated an assay for the detection and quantification of miRNA targets in total RNA samples. The assay is based on an ITP process which selectively focuses miRNA and MB into an order 10 pL zone, in which we perform and analyze MB hybridization. We showed that ITP hybridization enables length-selective detection of miRNA and can distinguish miRNA from its precursors. We also showed that the sequence specificity of MBs was unaffected by coupling hybridization with ITP. Finally, we demonstrated the efficacy of the assay for the detection of miRNA targets in total RNA. We successfully detected miR-122 in liver and corroborated reduced expression in kidney. Using calibration experiments, we calculated the amount of miR-122 in liver, and our estimate is in fair agreement with measurements performed with other quantification methods. ITP hybridization is a fast (<2 min), low component cost (~$50 per chip, standard epifluorescence microscope and power supply, ~$0.50 of reagents per 100 runs), and sensitive (down to 3000 copies per cell) microfluidic method for miRNA profiling that requires small amounts of sample (100 ng of total RNA) with about a three-decade dynamic range. Its speed, automation, and low sample consumption make it an attractive alternative to PCR or Northern blot analysis. We hypothesize that further optimization of ITP and MB chemistries and dynamics could significantly enhance sensitivity and reach the 100 copies per cell level. We also hypothesize that ITP hybridization can be extended to the detection and quantification of any type of nucleic acids, for example RNA, rRNA, or genomic DNA.

## ASSOCIATED CONTENT

**Supporting Information.** Additional information as noted in the text. This material is available free of charge via the Internet at http://pubs.acs.org.

## AUTHOR INFORMATION

**Corresponding Author**
*E-mail: juan.santiago@stanford.edu.

## ACKNOWLEDGMENT

We gratefully acknowledge the support of the National Science Foundation under contract no. CBET-0729771-002.

## REFERENCES

(1) He, L.; Hannon, G. J. *Nat. Rev. Genet.* **2004**, *5*, 522–531.
(2) Lu, J.; Getz, G.; Miska, E. A.; Alvarez-Saavedra, E.; Lamb, J.; Peck, D.; Sweet-Cordero, A.; Ebet, B. L.; Mak, R. H.; Ferrando, A. A.; Downing, J. R.; Jacks, T.; Horvitz, H. R.; Golub, T. R. *Nature* **2005**, *435*, 834–838.
(3) Tricoli, J. V.; Jacobson, J. W. *Cancer Res.* **2007**, *67*, 4553–4555.
(4) Baker, M. *Nat. Methods* **2010**, *7*, 687–692.
(5) Wark, A. W.; Lee, H. J.; Corn, R. M. *Angew. Chem., Int. Ed.* **2008**, *47*, 644–652.
(6) Linsen, S. E. V.; de Wit, E.; Janssens, G.; Heater, S.; Chapman, L.; Parkin, R. K.; Fritz, B.; Wyman, S. K.; de Bruijn, E.; Voest, E. E.; Kuersten, S.; Tewari, M.; Cuppen, E. *Nat. Methods* **2009**, *6*, 474–476.
(7) Chen, C. F.; Ridzon, D. A.; Broomer, A. J.; Zhou, Z. H.; Lee, D. H.; Nguyen, J. T.; Barbisin, M.; Xu, N. L.; Mahuvakar, V. R.; Andersen, M. R.; Lao, K. Q.; Livak, K. J.; Guegler, K. J. *Nucleic Acids Res.* **2005**, *33*, 9.
(8) Varallyay, E.; Burgyan, J.; Havelda, Z. *Nat. Protocols* **2008**, *3*, 190–196.
(9) Tyagi, S.; Kramer, F. R. *Nat. Biotechnol.* **1996**, *14*, 303–308.
(10) Santangelo, P. J.; Nix, B.; Tsourkas, A.; Bao, G. *Nucleic Acids Res.* **2004**, 32.
(11) Everaerts, F. M.; Beckers, J. L.; Verheggen, T. P. E. M. *Isotachophoresis: theory, instrumentation, and applications*; Elsevier Scientific Pub. Co.: Amsterdam, 1976.
(12) Persat, A.; Marshall, L. A.; Santiago, J. G. *Anal. Chem.* **2009**, *81*, 9507–9511.
(13) Jung, B.; Bharadwaj, R.; Santiago, J. G. *Anal. Chem.* **2006**, *78*, 2319–2327.
(14) Hirokawa, T.; Yoshioka, M.; Okamoto, H.; Timerbaev, A. R.; Blaschke, G. *J. Chromatogr., B* **2004**, *811*, 165–170.
(15) Khurana, T. K.; Santiago, J. G. *Anal. Chem.* **2008**, *80*, 279–286.
(16) Schoch, R. B.; Ronaghi, M.; Santiago, J. G. *Lab Chip* **2009**, *9*, 2145–2152.
(17) Persat, A.; Chivukula, R. R.; Mendell, J. T.; Santiago, J. G. *Anal. Chem.* **2010**, *82*, 9631–9635.
(18) Park, C. C.; Kazakova, I.; Kawabata, T.; Spaid, M.; Chien, R. L.; Wada, H. G.; Satomura, S. *Anal. Chem.* **2008**, *80*, 808–814.
(19) Persat, A.; Morita, T.; Santiago, J. G. *Proc. MicroTAS* **2007**, *11*, 56–58.
(20) Goet, G.; Baier, T.; Hardt, S. *Lab Chip* **2009**, *9*, 3586–3593.
(21) Bercovici, M.; Kaigala, G. V.; Liao, J. C.; Santiago, J. G. *Proc. MicroTAS* **2010**, *14*, 797–799.
(22) Bocek, P.; Deml, M.; Janak, J. *J. Chromatogr., A* **1978**, *156*, 323–326.
(23) Khurana, T. K.; Santiago, J. G. *Anal. Chem.* **2008**, *80*, 6300–6307.
(24) Squires, T. M.; Quake, S. R. *Rev. Mod. Phys.* **2005**, *77*, 977–1026.
(25) Marras, S. A. E.; Kramer, F. R.; Tyagi, S. *Nucleic Acids Res.* 2002, *30*, e122.
(26) Straus, N. A.; Bonner, T. I. *Biochim. Biophys. Acta* **1972**, *277*, 87–95.
(27) Dubertret, B.; Calame, M.; Libchaber, A. J. *Nat. Biotechnol.* **2001**, *19*, 365–370.
(28) Barron, A. E.; Sunada, W. M.; Blanch, H. W. *Electrophoresis* **1996**, *17*, 744–757.
(29) Although here we have not shown single base specificity.
(30) Chang, J.; Nicolas, E.; Marks, D.; Sander, C.; Lerro, A.; Buendia, M. A.; Xu, C.; Mason, W. S.; Moloshok, T.; Bort, R.; Zaret, K. S.; Taylor, J. M. *RNA Biol.* **2004**, *1*, 106–13.
(31) Sarasin-Filipowicz, M.; Krol, J.; Markiewicz, I.; Heim, M. H.; Filipowicz, W. *Nat. Med.* **2009**, *15*, 31–33.
(32) Becker, C.; Hammerle-Fickinger, A.; Riedmaier, I.; Pfaffl, M. W. *Methods* **2010**, *50*, 237–243.
(33) Ach, R.; Wang, H.; Curry, B. *BMC Biotechnol.* **2008**, *8*, 69.